Hydrological Dynamics and Geo-Hazard Risks: A Case Study of Cikamiri Sub-Watershed

Soerya, S. F.,[1*] Asdak, C.,[1] Kendarto, D. R.[1] and Razali, N.[2]
[1]Faculty of Agro-industrial Technology, Universitas Padjadjaran, Indonesia
E-mail: sarah.f.soerya@unpad.ac.id,[*] ORCID ID: 0000-0003-2894-4639
[2]Environmental Engineering Technology, Universiti Kuala Lumpur, Malaysia
**Corresponding Author*

DOI: https://doi.org/10.52939/ijg.v22i5.4983

Abstract
Hydrological dynamics occur as a result of massive land cover changes in the Cikamiri sub-watershed, Garut, Indonesia. Changes in the hydrological patterns increase the frequency of hydrometeorological hazards in the Garut region. This study aims to analyse water balance dynamics and multi-disasters in data-scarce regions by integrating the FJ Mock model, Revised Universal Soil Loss Equation (RUSLE) and Flash Flood Potential Index (FFPI). Rainfall and spatial data from 2016 to 2025 were used to simulate the relation between water availability and land vulnerability with soil and rock types. The results show a decrease in Soil Moisture Capacity (SMC), resulting in weak watershed retention functions. The average discharge of the Cikamiri Sub-watershed 69.8 mm/month with high surface runoff and a combination of high erosion rates severe creates zones of significant landslide and flash flood vulnerability in the Cikamiri River flow. The results of the FFPI integration show a high concentration of vulnerability zones in areas with steep slopes and non-vegetation cover of 17.12% or 1,070.23 ha. This vulnerability affects the downstream area of the Cikamiri River, which flows into the Cimanuk River Basin. The geo-hazard modelling is consistent with the history of disasters in the study area, which were triggered by sediment accumulation and extreme peak discharge. Slope direction and contour analysis serve as the final validation of the analysis. The findings indicate the need for river basin management focused on the upstream and downstream areas of the Cikamiri sub-watershed, with improvements to drainage infrastructure and control of land clearing in the catchment area. The study provides a basic spatial framework for local governments in developing spatial risk-based development policy planning.

Keywords: Cikamiri Sub-Watershed, Flood Vulnerability, FJ Mock Model, Flash Flood Potential Index, Integrated Geo-hydrometeoroligical

1. Introduction

Urbanization is a significant factor influencing land cover change, particularly in tropical watersheds [1]. The Oshiwara River in Mumbai serves as a case study, illustrating that urban development has expanded by 75%, accompanied by a 43% reduction in open space. This has led to a substantial increase in inundation and flood zone areas, exceeding 20% [2]. Urbanisation and deforestation, by removing vegetation and modifying slopes, increase landslide susceptibility by up to 20% more than the effect of increased rainfall intensity [3]. Slope inclination, extreme rainfall and land cover that cannot withstand infiltration increase the potential for hydrometeorological disasters, particularly landslides [4]. Research conducted in Italy and Colombia has demonstrated a correlation between landslides in upstream regions and the subsequent occurrence of flooding downstream, leading to the formation of flash floods. This phenomenon, characterised by the occurrence of landslides that are unable to be contained due to heavy rainfall, results in flash floods within small to medium-sized watersheds [5][6] and [7]. The Gianh River Basin in Vietnam serves as a prime example of the interplay between floods and landslides during the rainy season, which often culminates in protracted disasters. These disasters are precipitated by landslides that generate sediment, thereby contributing to the augmentation of overflowing rivers [8]. Indonesia has a tropical climate similar to Vietnam. Furthermore, the significant growth population in Indonesia led to extensive land-use changes that impact the hydrological patterns.

Indonesia has experienced rapid population growth and significant changes in land cover, which have been found to be generally proportional

especially The island of Java [9]. Garut Regency, West Java, is located in several river basins and has experienced significant urbanisation and land cover change. Research conducted about land-use change over an eight-year period, the results found that the Cimanuk-Copong watershed in Garut Regency experienced an 8% increase in residential land cover, a 1.96% increase in buildings, and a 17% increase in plantations (Table 1). The overall change in land use in Garut Regency from 2007 to 2016 [10]. Land cover changes in the Garut region have drastically altered the hydrological regime, particularly in the Cimanuk watershed. This data is supported by land cover scenario data for 2000-2020, which shows an increase in runoff entering the Upper Cimanuk of 23.7% to 32.2% on a 2-25 year scale [11]. As a result of land use changes, the Cikamiri River Basin, located upstream of the Cimanuk River Basin, experienced an increase in water level with above-normal flow rates, causing the volume of water at the mouth of the Cikamiri River to increase and resulting in flooding [12]. Hydrometeorological disasters occur repeatedly and cause significant losses.

In 2011, flash floods swept away three houses in the village of Simpang. The impact of land cover change is becoming increasingly severe. Reaching its peak in 2023, flash floods in Garut Regency carried rocks and mud, cutting off the regency road at the location of the incident, rendering it completely impassable. The flash flood impact during 2011 to 2023 is presented in Table 2. This disaster is clear evidence of the failure of the watershed ecosystem to respond to rainfall. The Cikamiri sub-watershed has been identified as a major contributor to peak discharge, which triggers flash floods in Garut Regency, because it is located upstream and has undergone significant land cover change with a high percentage of slope inclination [13][14] and [15] it is noted that the change from vegetated to non-vegetated land cover has an impact on soil infiltration capacity and the volume of rainfall runoff. Based on research, [16] Rainfall distribution in the Cikamiri watershed is uneven; rainfall in the upstream area can cause increased river discharge in the downstream area. Monthly rainfall in the upstream Cimanuk watershed fluctuates between 18.2 and 366.5 mm/month [17]. As of 2017, changes in the Cimanuk watershed area have caused an increase in runoff and a decrease in baseflow contribution, indicating a higher flow regime and a rapid response to rainfall [18]. Monitoring of hydrometeorology in the Cikamiri sub-watershed area is still limited to manual water level data, while water balance dynamics and spatial risk mapping using physical parameters of the area's soil and slope are still very minimal. Early warning of hydrometeorological disasters is very difficult in the Cikamiri sub-watershed area, which has been identified as a contributor to potential hydrometeorological disasters in Garut Regency.

Most research on the Upper Cimanuk River Basin, particularly the Cikamiri Sub-Watershed, has focused on a single aspect that does not represent the entirety of integrated hydrometeorological disasters. A multi-hazard approach at the river basin scale, combining the principles of hydrology and river basin geomorphology, can improve the early warning system for hydrometeorological disasters [19]. Hydrometeorology depends on peak discharge values and water availability in a river basin, which correlates with a land area's ability to store water [20]. FJ Mock is a simple rainfall-runoff model based on water balance for tropical regions with limited data on river basins [21]. The FJ Mock method can be used as a water (hydrological) database for determining integrated landslide and flood potential using scoring methods and the Flash Flood Potential Index (FFPI).

Table 1: Cimanuk watershed land-use change [22]

Land-Use Category	Area in 2007 (ha)	Area in 2016 (ha)	Change (ha)	Remarks
Dryland Agriculture	2,430.61	770.98	-1,659.63	Significant Decrease
Irrigated Land	1,926,78	2,064.18	+137.40	Increase
Residential Areas	1,728,56	1,816.38	+87.82	Increase

Table 2: Summary of measured impacts

Year	Disaster Type	Human Impact	Material/Physical Impact	Estimated Economic Loss	Source
2011	Flash Flood	-	3 houses swept away	-	[12]
2014	Flash Flood	-	720 houses submerged; 7 swept away; 35 damaged	-	[23]
2016	Flash Flood & Mudslide	34 dead; 19 missing	Massive damage across 6 sub-districts	IDR 288 billion	[24]
2023	Debris Flow	-	6m x 20m retaining wall collapse; Regency Road cut off	-	[25]

The weighting of landslide cause factors is used to combine historical data (solid material side of sedimentation potential), vulnerability indicators and performance indices so that it is not just a weighting value [26]. FFPI is used to determine the basic vulnerability of an area to flash floods caused by rainfall occurring at that time [27]. FPPI is used because it is capable of integrating static physical parameters (slope gradient, soil type) with dynamic parameters (rainfall and/or discharge). The integration of these three methods involves changes in land cover and hydrological dynamics that are rarely found in river basin areas in West Java Province, Indonesia. Therefore, this hydrometeorological dynamics analysis offers a spatial integration approach that is expected to provide early warning information on multiple hazards at the watershed scale and support spatial planning in Garut Regency.

2. Material and Methods

This analysis is divided into three main phases, namely water availability estimation, land degradation analysis, and flash flood hazard modelling. The study area is located in the Cikamiri Sub-DAS, Garut Regency, West Java, Indonesia (Figure 1), covering an area of 6,258.68 ha. Geographically, the Cikamiri Sub-Watershed is located at 7° 7′ 30″S to 7° 15′ 0″S and 107° 41′ 30″E to 107° 54′ 0″E. The conditions of the watershed is presented in Figure 2.

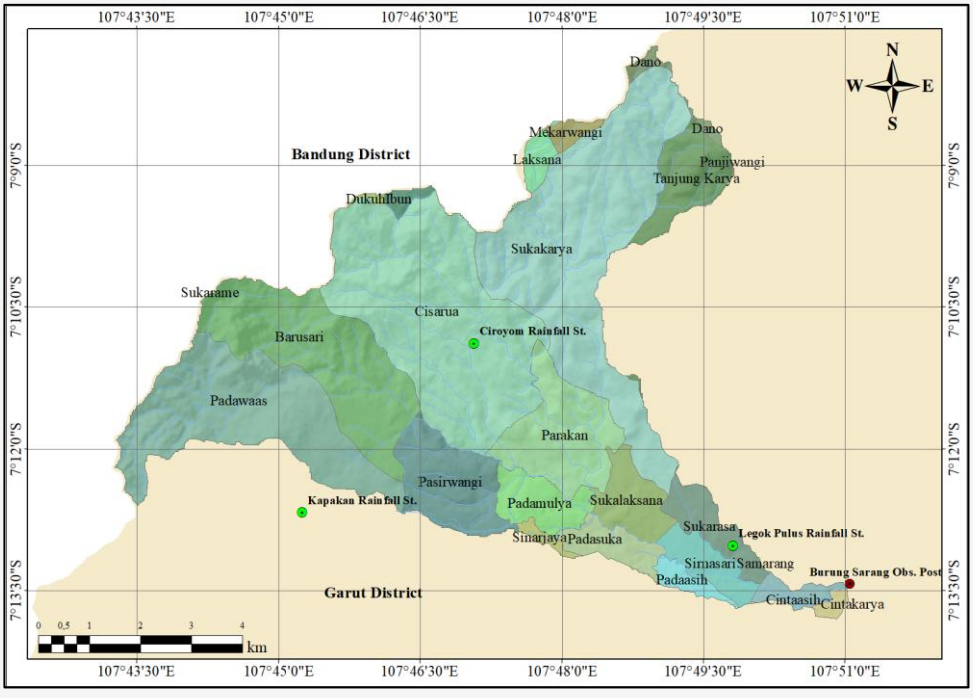

Figure 1: Administration of the Cikamiri Sub-watershed

Figure 2: Current conditions of the Cikamiri Sub-watershed

2.1 Water Table Balance and Discharge Analysis

The FJ. Mock method was used to estimate discharge. The method is divided into eight main steps as follows [28] and [29]:

1) Eastimation of potential evapotranspiration (E_p)
2) Estimation of actual evapotranspiration (E_a)
3) Determining the amount of rain at ground level (D_s)
4) Determining the amount of soil moisture (SMC)
5) Determining infiltration (i), between 0-1
6) Determining excess water in soil (water surplus)
7) Determining groundwater content (V_n)
8) Determining changes in groundwater content (DV_n)
9) Estimation of total runoff which accumulate base flow, direct runoff, and storm runoff.

2.2 Data Source

Data required to estimate water availability using the FJ. Mock method in Table 3, and the parameters used in FJ Mock are listed in Table 4.

Soil Moisture Capacity, the maximum capacity of soil to store water before it becomes surface runoff or groundwater. If precipitation > SMC, then SRO = 0; if precipitation < SMC, then SRO = precipitation multiplied by the percentage factor. Rainfall is part of the hydrological cycle and is one of the most important components in determining the surface runoff coefficient. [30]. Rainfall values can be calculated using data from climatological stations close to the research location. To ensure that there are no errors in the hydrological data, data consistency tests can be carried out on the existing data results. Data consistency tests can be carried out using various methods, one of which is the RAPS (Rescaled Adjusted Partial Sums) method [31].

2.3 Total Runoff Calculation

Total Runoff is the accumulation of base flow, direct runoff and storm runoff. Total runoff (TRO) is determined using Equation 1:

$$TRO = BF + DRO + SRO$$

Where:

BF = base flow (m³/s/km)
DRO = Direct runoff (Total Runoff) (mm/month)
WS = Water surplus
SRO = Storm runoff (mm/month)
TRO = Runoff for period n (m³/s/km²)

Table 3: Data source

No	Material	Description	Source
1	Climatology Data (temperature, sunlight, wind speed)	Evapotranpiration data Year 2016 – 2025	Metereology, Climatology and Geophysiscs Agency of Indonesia
2	Rainfall Data	Year 2016-2025	from Metereology, Climatology and Geophysics Agency of Indonesia
3	Digital Elevation Model Data	Slope and Relief Data for Interpretation	Peta Rupa Bumi Indonesia (Indonesian Topographical Map) renewed by *Google Earth* 2025
4	Land Cover Map	2016 and 2025 Land Cover Map	Peta Rupa Bumi Indonesia (Indonesian Topographical Map) renewed by *Google Earth* 2025
5	Soil Sample	Soil texture, organic matter and soil permeability	Primary data
6	Statistic Data	Population growth data 2016 - 2025	Indonesian Central Bureau of Statistics

Table 4: FJ Mock parameter [32][33] and [34]

No	FJ Mock Parameter	Symbol	Unit
1	Percentage Factor	*PF*	%
2	Infiltration Coefficient	*if*	-
3	Soil Moisture Capacity	*SMC*	mm
4	Exposed Surface	*m*	%
5	Initial Groundwater Storage	*IGS*	mm
6	Recession Constant	*k*	-

2.4 Discharge Calculation

Calculation of discharge based on the F.J Mock method is defined in Equation 2:

$$Q_n = TRO \times CA$$

Equation 2

Where:

Q_n = Amount of water available from the source (m^3/s)
TRO = Total Runoff (mm/month)
CA = Catchment area (km^2)

2.5 Land Degradation and Erosion Modelling

The RUSLE method uses four calculated factors, namely rainfall erosivity or surface runoff, soil erodibility, slope gradient, crop management and conservation [36], which are classified into erosion hazard classes (very low – very high) for conservation planning [36]. Calculation method expressed in Equation 3:

$$A = R \times K \times LS \times CP$$

Equation 3

Where A is the average annual soil loss ($t.ha^{-1}.year^{-1}$); R is the rainfall erosivity factor [M] $mmh^{-1}.ha^{-1}.year^{-1}$, rainfall erosivity factor obtained from calculations of high rainfall intensity over 10 years [35] from the rainfall station in the Cikamiri sub-watershed; K is the soil erodibility factor [metric tons ha^{-1}. Mj^{-1} mm^{-1}] obtained from soil texture testing samples; LS = slope length steepness factor, (ranges 0–1) obtained from DEMNAS (Digital Elevation Model Nasional); LS constructed from digital elevation model (DEM); and CP is the practice support of land management (without measurements ranging from 0–1) [36].

2.6 Surface Runoff and Landslide Asessment

Landslide susceptibility (LS) is influenced by the factors namely rainfall (F_r), rock type (F_{rt}), slope length (F_s), land cover (F_{lc}) and soil type (F_{st}). Lanslide susceptibility map can be created from overlaying all the five parameters susing map overlay technique. In this study, Equation 4 is used to create the landslide susceptibility map [37].

$$LS = 0.3\ F_r + 0.2\ F_{rt} + 0.3\ F_s + 0.2\ F_{lc} + 0.1\ F_{st}$$

Equation 4

The empirical parameter used to express the runoff potential of an area is called the Curve Number (CN) [38] The weighted CN value is obtained by multiplying the land cover area by the HSG, and the composite CN value is calculated by dividing the weighted CN by the total watershed area [39]. Meanwhile, impervious refers to impermeability, or the area that is impermeable or unable to absorb water or AMC [40].

2.7 Integrated Flash Flood Potential Indesx (FFPI)

The FFPI index assessment in this study used the FFPI method developed by [41] research in the Tamiang River Basin in Aceh, which is the latest research in Indonesia to use the FFPI method in analysing the potential for flash flooding. Given the similar tropical conditions, it is assumed that the research area has similar conditions. The first step was to reclassify the parameters of flash flood vulnerability based on the FPPI index assessment. The FFPI index values for each parameter were then processed using ArcGIS 10.4 software with the Weighted Overlay Analysis method using the FFPI value determined from Equation 5. The weighting of each parameter is shown in Table 5.

$$FFPI = \frac{16FKL + 34.1FAPI + 34.9FCN + 8.4FRGT}{100}$$

Equation 5

Where:

FFPI = Flash Flood Potential Index
FKL = FFPI Slope
FAPI = FFPI API
FCN = FFPI Curve Number
FRGT = FFPI Landslide Prone

Table 5: FFPI classes and weights

Factor	Weights	Classes	FFPI Score
Slope	16	0-8%	1
		8-15%	2
		15-25%	3
		25-40%	4
		>40%	5
API	34.1	0-100 mm	1
		100-150 mm	3
		>150 mm	5
Curve Number	34.9	0-30	1
		30-60	3
		60-100	5
Land Movement	8.4	Low	1
		Medium	3
		High	5
United Lithology	6.5	Frozen	1
		Metamorphic	3
		Sedimentary	5

Land movement is taken from the cumulative score of landslides. The FFPI Index values produced in this study range from 1 to 5, representing each classification of flash flood vulnerability (very low to very high) [42].

The results of this assessment are presented in the form of a flash flood vulnerability map with specific scales and colours to clarify the elements displayed.

2.6 Spatial Justification and Flow Analysis

Justification was carried out to add the factor of regional influence with high and moderate flash flood vulnerability levels to the areas below that are located on the slope. Justification was carried out by comparing historical data on previous flash floods [43]. This stage was carried out using slope direction maps, contours and river boundaries to adjust land use in the Cikamiri sub-watershed. The analysis results used DEMNAS data to determine the direction of flow in the event of flooding.

3. Results and Discussion

Land cover changes over the past 10 years, from 2016 to 2025, are illustrated in Figure 3. The Cikamiri sub-watershed shows variability in land cover or land use, which includes irrigated rice fields, fields, mixed crops, water and agricultural structures, residential and office buildings, and vacant land. The largest change was in rice fields, which increased by 2.87% of the total area of the Cikamiri sub-watershed or 31.54 ha, followed by food production needs in Garut Regency. Settlements were the second largest change, at 14.28 ha or 1.30% of the total area of the Cikamiri sub-watershed. Settlements are growing larger with population growth and the need for other buildings for education, health, accessibility, and other supporting buildings to improve community welfare. The increase in rice field and settlement area is an important indicator in spatial planning and land cover prediction, showing the dynamics between food needs and the need for permanent residence [44] which must be managed to maintain soil and water conservation principles and mitigate the risk of hydrometeorological disasters.

3.1 Rainfall and Water Balance

Rainfall in the Cikamiri sub-watershed was obtained from three stations, namely Kapakan Station, Ciroyom Station and Legok Pulus Station, using the Thiessen method to obtain the average rainfall for the area. The largest area of influence was dominated by the Ciroyom Rainfall Station. The distribution of rainfall in the Cikamiri Sub-DAS is illustrated on the map in Figure 4. The analysis of average rainfall data from 2016 to 2025 shows that the highest monthly rainfall occurs in February at 374 mm/month and the lowest average in August at 69.8 mm/month. There is a significant difference between the month with the highest rainfall and the month with the lowest rainfall, namely 304.2 mm/month. Rainfall is one component of the water cycle, when it falls directly evaporates before reaching the earth's surface (soil) [45]. High rainfall accumulation creates high antecedent moisture conditions, keeping the soil wet for a long time and reducing the interval between rainfall and runoff. The exceptionally high rainfall in February triggered historic flash floods in Garut Regency. The weights of 0.3 for the rainfall in Table 6 was assigned based on the role of triggering factor in FFPI [46]. Rainfall distribution shows that rainfall intensity creates a large hydrological load on river systems from the point of origin. Rainfall increases from upstream to downstream, with distribution influenced by topography and monsoons that produce extreme rainfall intensity [47]. In headcut or gully systems, increased inflow from upstream increases the potential and kinetic energy of the flow, causing erosion that correlates strongly with an increase in sediment trapped downstream [48].

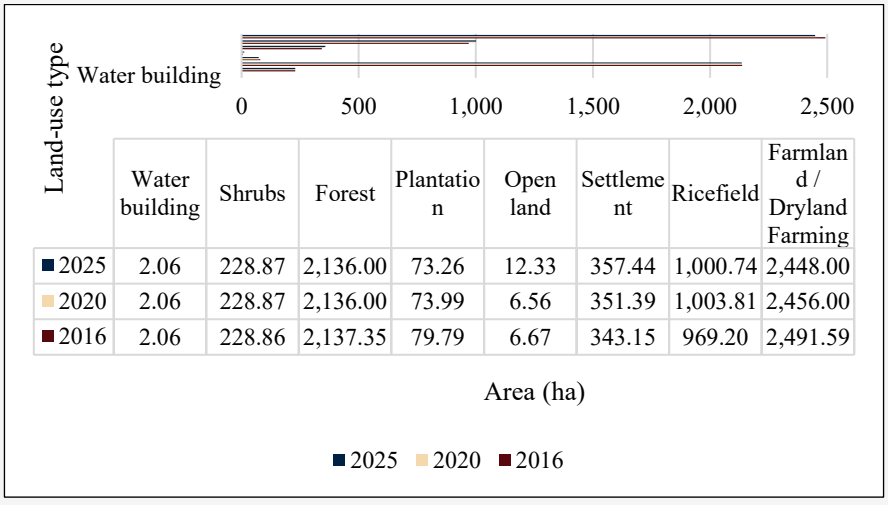

	Water building	Shrubs	Forest	Plantation	Open land	Settlement	Ricefield	Farmland / Dryland Farming
2025	2.06	228.87	2,136.00	73.26	12.33	357.44	1,000.74	2,448.00
2020	2.06	228.87	2,136.00	73.99	6.56	351.39	1,003.81	2,456.00
2016	2.06	228.86	2,137.35	79.79	6.67	343.15	969.20	2,491.59

Figure 3: Graph of land cover change in the Cikamiri Sub-watershed area from 2016 to 2025

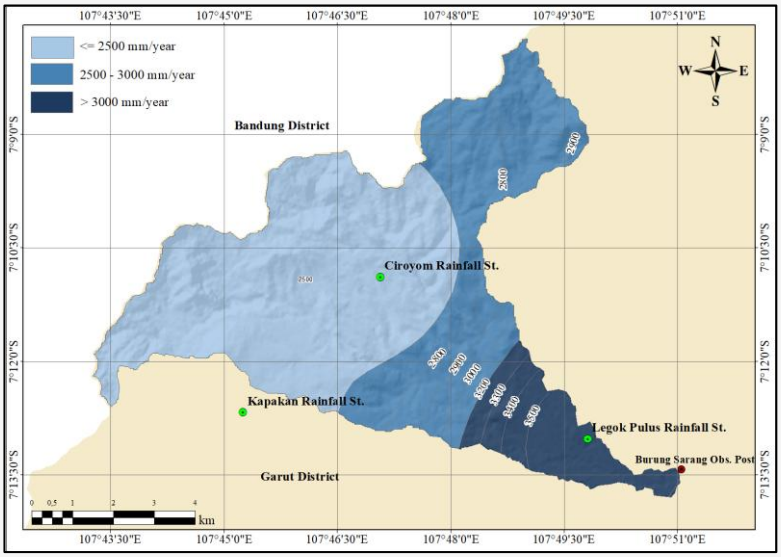

Figure 4: Rainfall distribution of the Cikamiri Sub-watershed

Table 6: Rainfall in the Cikamiri sub-watershed

Rainfall (mm/year)	Classification	Score	Weights	Final Score	Area (Ha)	Percentage (%)
< 2,500	Moderately wet	3		0.9	1,983.57	31.69
2,501– 3,000	Very wet	4	0.3	1.2	3,354.32	53.59
> 3,000	Extremely wet	5		1.5	920.79	14.71
				Total	**6,258.68**	**100.00**

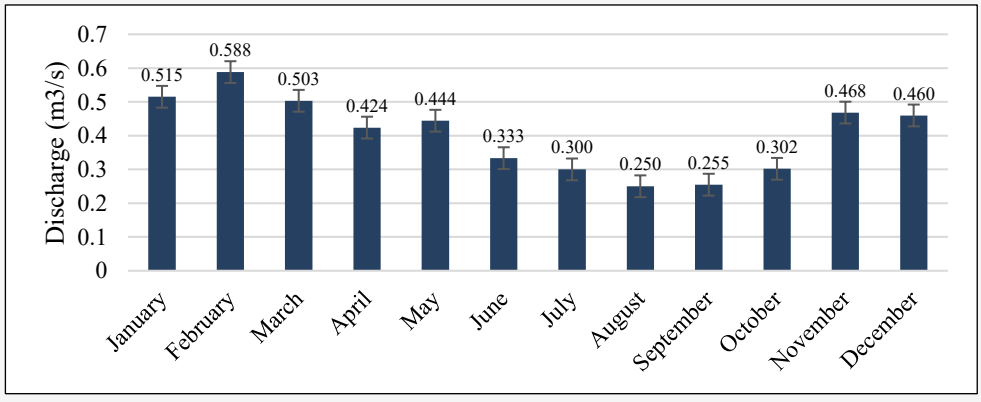

Figure 5: Fluctuations discharge in Cikamiri Sub-watershed

The 1.46 mm decrease in SMC reflects a reduction in soil voids due to the conversion of land cover to built-up land, which causes the soil to reach saturation point more quickly. Extreme rainfall in February coincided with declining SMC, and the soil was unable to infiltrate water optimally. As a result, the rain was directly converted into massive surface runoff. According to Figure 5, it was found that the highest average discharge occurred in February at 0.588 m^3/s. The lowest discharge occurred in August at 0.25 m^3/s. August was the driest month, as indicated by the high evapotranspiration and low water surplus and runoff. The historical condititaons of the Cikamiri sub-watershed have caused rainwater to no longer be released slowly as baseflow, but rather simultaneously as destructive peak discharge at the mouth of the Cikamiri River. This peak and low discharge align with monsoonal rainfall patter in West Java. Northwest Monsoon brings maximum precipitation between December-February and dry season between June-August [49]. Land degradation reduces the watershed's natural regulation capacity [50].

3.2 Physical Characteristics of River Basin

The physical characteristics of a river basin are its slope, soil and rock. Figures 6 to 8 show the distribution of the physical characteristics of the Cikamiri sub-watershed. Slopes with a gradient of 15-30% (moderately steep) cover the largest area in the Cikamiri sub-watershed, with an area of 2,388.99 ha or 38.17% of the total area, with the most moderately steep slopes in the upstream area. The downstream area is mostly flat, which is a factor in the potential for sediment and flooding to accumulate in the downstream area. Moderate slope gradients are most prevalent in the headwaters, increasing the surface runoff factor on agricultural land cover and buildings. The rock types in the Cikamiri Sub-DAS are dominated by Rakutak volcanic rock (Qpr3) of the Breccia, Andesite-Basalt type, covering an area of 3,371.50 ha, which is 53.87% of the total area of the Cikamiri Sub-DAS. Volcanic rocks are highly susceptible to landslides due to their tendency to be brittle and prone to damage. When subjected to shock or pressure changes, volcanic rocks can crack and break easily, increasing the risk of landslides [51]. The dominant soil type in the Cikamiri Sub-DAS area is Kambisol, covering a total area of 4,629.18 ha or 73.6% of the total area of the Cikamiri Sub-DAS, indicating that almost three-quarters of the Cikamiri Sub-DAS area is Kambisol soil. Kambisol soil is prone to landslides due to its unstable structure and low organic content [52]. The combination of slopes, easily eroded rock and saturated soil types creates a mechanism for concentrated water flow in river valleys.

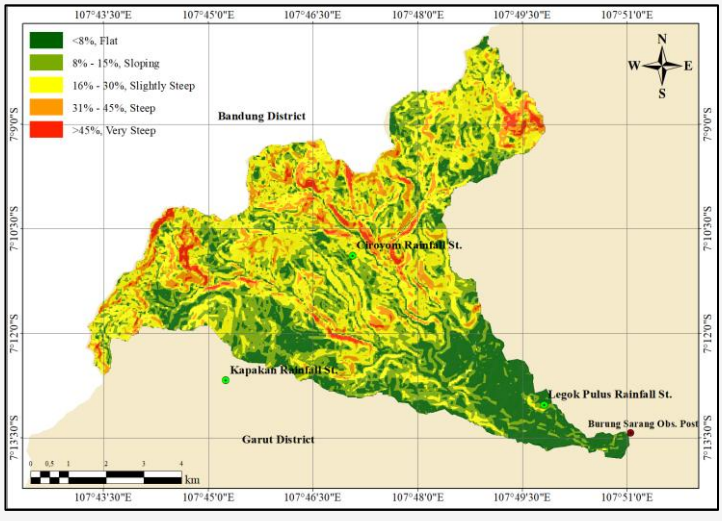

Figure 6: Slope of Cikamiri Sub-watershed

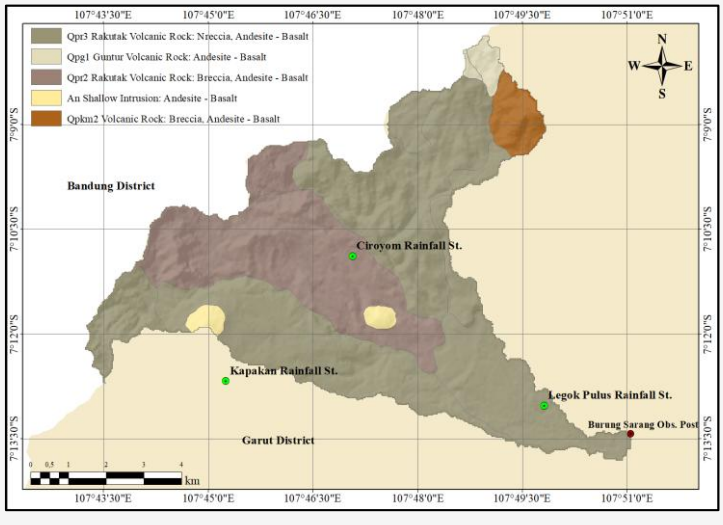

Figure 7: Rock type of Cikamiri Sub-watershed

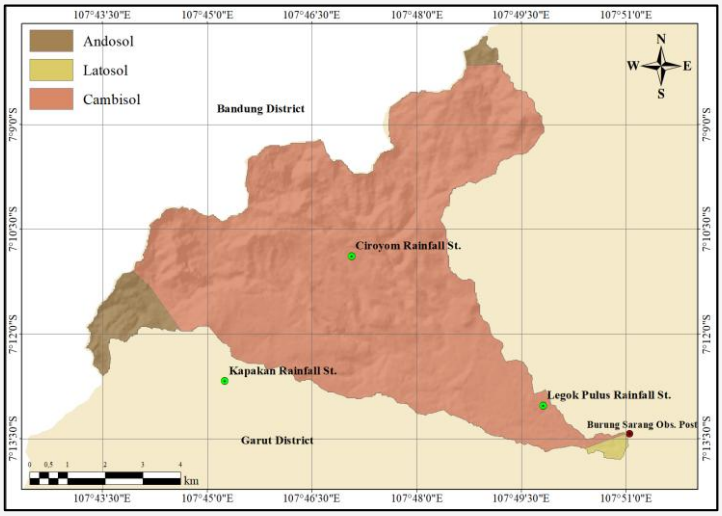

Figure 8: Soil type of Cikamiri Sub-watershed

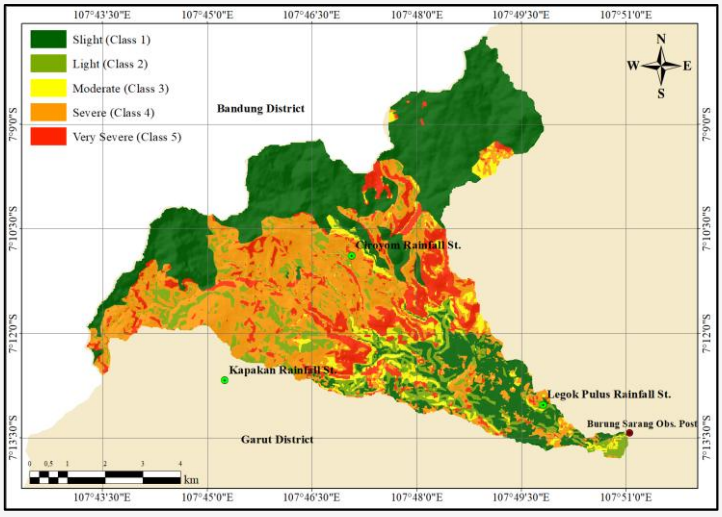

Figure 9: Erosion rate vulnerability of Cikamiri sub-watershed

3.3 Analysis of Erosion and Erosion Vulnerabilityas Sediment Providers

Based on surface runoff parameters, slope gradient, soil type and land cover, the distribution of erosion potential is shown in Figure 9. The RUSLE modelling results show land cover degradation in non-forest upstream areas, mainly settlements or open land, and that the middle area has a severe erosion potential of 34.83% of the Cikamiri sub-watershed area, or 2,179.6 ha (Table 7). The erosion rate of the Cikamiri sub-watershed reached 38.55 tonnes/ha/year, six times higher than the T-Value of cambisol soil, which is 3.08 – 15.42 tonnes/ha/year [53]. The main factor in the percentage of erosion potential is triggered by crop management and dry agricultural land (C- Factor). The erosion potential triggers a significant rate of soil loss, exceeding the permissible erosion limit. The high erosion rate provides a potential sediment load, and when peak discharge occurs, the sediment will be transported. The sediment increases the viscosity of the water and transforms the flood into a debris flow (mudslide). A smaller SMC value reduces the soil's ability to absorb water and increases the overland flow.

Table 7: Erosion rate vulnerability area of Cikamiri sub-watershed

Class	Description	Erosion Rate (ton/ha/year)	Area (ha)
I	Slight	<15	1,130.37
II	Light	15-60	1,004.31
III	Moderate	60-180	503.47
IV	Severe	180-840	2,179.96
V	Very Severe	>480	1,440.56
		Total	**6,258.68**

Table 8: Integrated geo-hazard area of Cikamiri sub-watershed

Class	Description	Score	Area (ha)
I	Minimal Risk	1-2	624.93
II	Low Risk	3-4	1,242.06
III	Moderate Risk	5-6	1,892.61
IV	High Risk	7-8	1,428.84
V	Extreme Risk	9-10	1,070.23
		Total	**6,258.68**

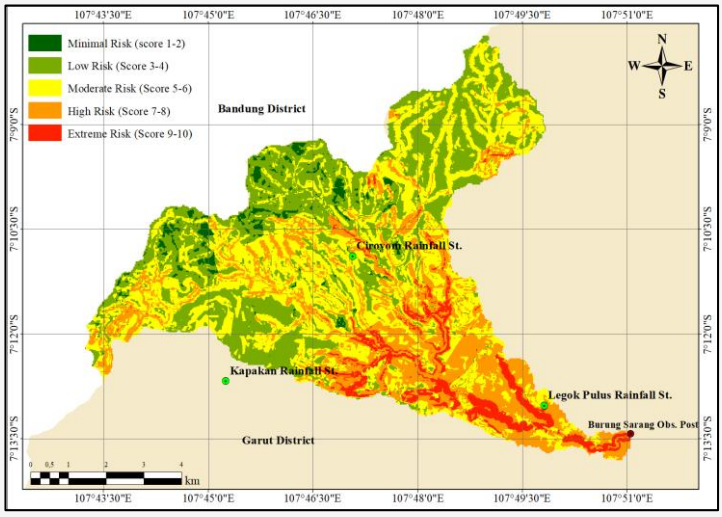

Figure 10: Integrated geo-hazard of Cikamiri sub-watershed

3.4 Integrated Geo-hazard Potential

The integration of slope stability parameters and hydrological dynamics produces a comprehensive multi-hazard risk map in Figure 10. The integration of geo-hydrometeoroligical parameter reveals that unstable slopes, erosion-causing sedimentation, high soil saturation levels and extreme rainfall in some parts of the region resulting the primary drivers of peak discharge. Zones with extreme risk are the result of an overlay between areas with high potential for landslides and vulnerability to flash floods. Based on the integration of extreme risks, the majority are concentrated in the middle-downstream of the Cikamiri Sub-DAS, mainly in the area along the Cikamiri River with non-vegetated land cover and slopes. Table 8 shows that the area of extreme risk reaches 17.12% or 1,070.23 ha. Flow path analysis confirms the topographical accumulation of risk towards the outlet of the Cikamiri Sub-DAS, ilustrating the potential for mudflow flash floods in residential areas downstream of the Cikamiri Sub-DAS. The accuracy of the model was validated by historical disasters in 2016 and 2023 [25] and [54]. Historical locations affected were in areas of extreme risk. This shows strong consistency in the points of most severe damage. The integrated geo-hazard map proves that the integration of geo-hydrometeorological parameters is capable of mapping critical points with precision for the purposes of disaster mitigation and spatial planning in Garut Regency and the Cimanuk River Basin.

4. Conclusions

Based on the comprehensive assesment of hydrological dynamics and geo-hazard risks in Cikamiri Sub-watershed, the study leads to the following primary conclusions and actionable management recomendations:

1. Cikamiri Sub Watershed's landuse change led to significant potential of geo-hydrometeoroligical or geo-hazard potential. Evidenced by the reduction of Soil Moisture Capacity from 153.54 mm to 152.08 mm. The interaction of extreme rainfall, steep slopes and fragile lithology aggravate geo-hazard risks, with severe erosion by 1,679.94 ha (26.84%) and provides a potential sediment load, transforms the flood into a debris flow (mudslide).
2. The integrated multi-hazard assessment identifies that the reaches 17.12% or 1,070.23 has extreme risks zone, with the highest vulnerability concentrated primarily along the main river corridors. The accuracy of this spatial model is further validated by the 2016 and 2023 historical disaster.

3. The ability to provide a spatial framework is a key aspect of this study, which can be replicated for disaster mitigation in areas with limited observational data (data-scarce regions). Geo-hazard potential maps serve as a crucial tool for local authorities to refine spatial planning and implement soil and water conservation strategies, thereby preventing potential flooding from turning into damaging or destructive mudslides.
4. The practical limitations of this study acknowledges that the analysis relies on model-based simulations in a regional context where data is scarce. Discharge estimates will be more accurate following further validation through continuous field measurements. Future research is advised to utilise climate change scenarios to dynamically project long-term risks and to integrate assessments of communities' socio-economic vulnerability to develop more holistic, community-based data-driven disaster prevention planning model.

Acknowledgements

The author gratefully thanks the Padjadjaran Postgraduate Scholarship for providing financial support, enabling the author to conduct research and publish this work. The author also thanks all those who assisted in the research, writing and publication process.

References

[1] Wiwoho, B. S., Phinn, S. and McIntyre, N., (2023). Two Decades of Land-Use Dynamics in an Urbanizing Tropical Watershed: Understanding the Patterns and Drivers. *ISPRS International Journal of Geo-information.* Vol. 12(3). https://doi.org/10.3390/ijgi12030092.

[2] Zope, P. E., Eldho, T. I. and Jothiprakash, V., (2016). Impacts of Land Use–land Cover Change and Urbanization on Flooding: A Case Study of Oshiwara River Basin in Mumbai, India. *Catena,* Vol. 145; 142–154. https://doi.org/10.1016/j.catena.2016.06.009.

[3] Bozzolan, E., Holcombe, E. A., Pianosi, F., Marchesini, I., Alvioli, M. and Wagener, T., (2023). A Mechanistic Approach to Include Climate Change and Unplanned Urban Sprawl in Landslide Susceptibility Maps. Science of The Total Environment, Vol. 858. https://doi.org.10.1016/j.scitotenv.2022.159412.

[4] Liu, Y., Deng, Z. and Wang, X., (2021). The Effects of Rainfall, Soil Type and Slope on the Processes and Mechanisms of Rainfall-Induced Shallow Landslides. *Applied Sciences,* Vol. 11(24). https://doi.org/10.3390/app112411652.

[5] Vega J., Ortiz-Giraldo L., Botero B. A., Hidalgo C. and Parra J. C., (2024). Probabilistic Cascade Modeling for Enhanced Flood and Landslide Hazard Assessment: Integrating Multi-Model Approaches in the La Liboriana River Basin. Water (Basel). Vol. 16(17). https://doi.org/10.3390/w16172404.

[6] Dolojan, N. L. J., Moriguchi, S., Hashimoto, M., Tinh, N. X., Tanaka, H. and Terada, K., (2023). Hydrologic-geotechnical Modelling of Shallow Landslide and Flood Hazards Caused by Heavy Rainfall. *Engineering Geology,* Vol. 323. https://doi.org/10.1016/j.enggeo.2023.107184.

[7] Bout, B., Lombardo, L., Van Westen, C. J. and Jetten, V. G., (2018). Integration of Two-phase Solid Fluid Equations in a Catchment Model for Flashfloods, Debris Flows and Shallow Slope Failures. *Environmental Modelling & Software,* Vol. 105; 1–16. https://doi.org/10.1016/j.envsoft.2018.03.017.

[8] Nguyen, H. D., Dang, D. K., Nguyen, Q. H., Phan-Van, T., Bui, Q. T., Petrisor, A. I. and Nghiem, S. V., (2024). Monitoring the Effects of Climate, Land Cover and Land Use Changes on Multi-hazards in the Gianh River Watershed, Vietnam. *Environmental Research Letters,* Vol. 19(10). https://doi.org/10.1088/1748-9326/ad7278.

[9] Kelly-Fair, M., Gopal, S., Koch, M., Pancasakti Kusumaningrum, H., Helmi, M., Khairunnisa, D. and Kaufman, L., (2022). Analysis of Land Use and Land Cover Changes through the Lens of SDGs in Semarang, Indonesia. *Sustainability,* Vol. 14(13). https:doi.org/10.3390/su14137592.

[10] Mardianti, F. and Permana, S., (2024). Analisis Perbandingan Debit pada Das Cimanuk-Copong Kabupaten Garut Akibat Perubahan Tata Guna Lahan [A Comparative Analysis of Discharge at the Cimanuk-Copong River Basin in Garut Regency Due to Changes in Land Use]. *JMTS: Jurnal Mitra Teknik Sipil,* Vol. 1; 215–228. https://doi.org/10.24912/jmts.v7i1.26048.

[11] Kamanda, A., Anggraheni, E. and X Kuncoro, E., (2024). Analysis of Land Cover Changes Impact on Design Flood Estimation Case study: Upper Cimanuk Watershed in Garut City. *IOP Conferen*ce Series Earth Environtmental Science, Vol. 1343(1). https://doi.org/10.1088/1755-1315/1343/1/012015.

[12] Yulizar, Y. and Asdak, C. ,(2025). The Joint Variation of Temperature and Precipitation Across Indonesia: a Seasonal and Regional Analysis. *Theoretical and Applied Climatology,* Vol. 156(11), 1-15. https://doi.org/10.1007/s00704-025-05872-7.

[13] Munggaran, G., Hidayat, Y., Tarigan, S. D. and Baskoro, D. P. T., (2019). Analisis Respon Hidrologi dan Simulasi Teknik Konservasi Tanah dan Air Sub DAS Cimanuk Hulu [Analysis of Hydrological Responses and Simulation of Soil and Water Conservation Techniques in the Upper Cimanuk Sub-Watershed]. *Jurnal Ilmu Tanah dan Lingkungan,* Vol. 19(1); 26–32. https://doi.org/10.29244/jitl.19.1.26-32.

[14] Muchtaranda, I. H., Sulistyowati, T. and Muhajirah, M., (2022). Pengaruh Hujan Terhadap Stabilitas Lereng Dengan Retakan Pada Tanah Kohesif [The Effect of Rainfall on the Stability of Slopes with Cracks in Cohesive Soil]. *Spektrum Sipil,* Vol. 9(2); 97–110. https://doi.org/10.29303/spektrum.v9i2.239.

[15] Susetyaningsih, A., (2012). Pengaturan Penggunaan Lahan Di Daerah Hulu Das Cimanuk Sebagai Upaya Optimalisasi Pemanfaatan Sumberdaya Air [Land Use Planning in the Upper Cimanuk River Basin as a Means of Optimising Water Resource Utilisation]. *Jurnal Konstruksi,* Vol. 10(01); 1-8. https://doi.org/10.33364/konstruksi/v.10-01.107.

[16] Syabana, T. A. A., (2018*). Implikasi Perubahan Tata Guna Lahan Terhadap Fluktuasi Debit di DAS Cikamiri Kabupaten Garut [The Impact of Land Use Change on Flow Fluctuations in the Cikamiri Catchment Area, Garut Regency],* Magister Thesis. Graduate School, Padjadjaran University.

[17] Permana, S. and Susetyaningsih, A., (2025). Analisis Karakteristik Curah Hujan Terhadap Banjir di Kabupaten Garut [Analysis of Rainfall Characteristics in Relation to Flooding in Garut Regency]. *Teras Jurnal: Jurnal Teknik Sipil,* Vol. 15(1); 201–212. https://doi.org.10.29103/tj.v15i1.1232.

[18] Ridwansyah, I., Yulianti, M., Apip, Onodera, S. I., Shimizu, Y., Wibowo, H. and Fakhrudin, M., (2020). The Impact of Land Use And Climate Change on Surface Runoff and Groundwater in Cimanuk Watershed, Indonesia. *Limnology (Tokyo),* Vol. 21(3); 487–498. https://doi.org/ 10.1007/s10201-020-00629-9.

[19] Dolojan, N. L. J., Moriguchi, S., Hashimoto, M., Tinh, N. X., Tanaka, H. and Terada, K., (2023). Hydrologic-Geotechnical Modelling of Shallow Landslide and Flood Hazards Caused by Heavy Rainfall. *Engineering Geology,* Vol. 323. https://doi.org/10.1016/j.enggeo.2023.107184.

[20] Sun, Z., Zhu, X., Pan, Y. and Zhang, J., (2017). Assessing Terrestrial Water Storage and Flood Potential Using GRACE Data in the Yangtze River Basin, China. *Remote Sening (Basel),* Vol. 9(10). https://doi.org/10.3390/rs9101011

[21] Triwibowo, D., Elma, M., Suhartono, E., Riduan, R. and Noor, I., (2025). Hydrological Modeling of Reclaimed Catchment Area and Pit Lake for the Management of Degraded Post-Mining Land. *Journal of Degraded and Mining Lands Management,* Vol. 12(4); 7901–7912. https://doi.org/10.15243/jdmlm.2025.124.7901

[22] Asdak, C. and Supian, S., (2018). Watershed Management Strategies for Flood Mitigation: A Case Study of Jakarta's Flooding. *Weather and Climate Extremes,* Vol. 21; 117-122. https://doi.org/10.1016/j.wace.2018.08.002.

[23] Yuniati, N., (2016). Banjir Bandang Garut Karena Alih Fungsi Lahan di Hulu Sungai Cimanuk [Flash Floods in Garut Caused by Land Use Change in the Upper Reaches of the Cimanuk River]. Pikiran Rakyat. [Online]. Available: https://www.pikiran-rakyat.com/jawa-barat/pr-01264394/banjir-bandang-garut-karena-alih-fungsi-lahan-di-hulu-sungai-cimanuk-380448. [Accessed: Nov. 05, 2025].

[24] Tejakusuma I. G., (2016). *Bencana Banjir Bandang di Garut 20 September 2016 [Flash Flood Disaster in Garut, 20 September 2016].* Jurnal Sains dan Teknologi Mitigasi Bencana, Vol 11(2);10–18.

[25] Garut District Government. *Banjir di 5 Kecamatan Kabupaten Garut [Flooding in 5 Sub-districts of Garut Regency]. Jabar Prov.* [Online]. Available: https://Jabarprov.Go.Id/Berita/Banjir-Di-5-Kecamatan-Kabupaten-Garut-8785. [Accessed, Nov. 01, 2025]

[26] Memisoglu Baykal, T., 2025. Performance Assessment of GIS-based Spatial Clustering Methods in Forest Fire Data. *Natural Hazards,* Vol. 121(7); 8445–8477. https://doi.org/10.1007/s11069-025-07135-0.

[27] Popa, M. C., Simion, A. G., Peptenatu, D., Dima, C., Draghici, C. C., Florescu, M. S. and Diaconu, D. C., (2020). Spatial Assessment of Flash-flood Vulnerability in the Moldova River Catchment (N Romania) using the FFPI. *Journal of Flood Risk Management,* Vol. 13(4). https://doi.org/10.1111/jfr3.12624.

[28] Lubis R. I. S., Syahrul S. and Devianti D., (2022). Penggunaan Model Mock dalam Menghitung Ketersediaan Air di Daerah Aliran Sungai (DAS) Krueng Aceh [The Use of the Mock Model in Calculating Water Availability in the Krueng Aceh River Basin]. *Jurnal Ilmiah Mahasiswa Pertanian,* Vol. 7(3); 322–331. https://doi.org/10.17969/jimfp.v7i3.20803.

[29] Chandrasasi, D., Montarcih Limantara, L. and Wulan Juni, R., (2020). Analysis Using the F. J. Mock Method for Calculation ff Water Balance in the Upper Konto Sub-Watershed. *IOP Conference Series: Earth and Environmental Science,* Vol. 437(1). https://doi.org/10.1088/1755-1315/437/1/012019.

[30] Muchtaranda, I. H., Sulistyowati, T. and Muhajirah, M., (2022). Pengaruh Hujan Terhadap Stabilitas Lereng Dengan Retakan Pada Tanah Kohesif [The Effect of Rainfall on the Stability of Slopes with Cracks in Cohesive Soil]. *Spektrum Sipil,* Vol. 9(2); 97–110. https://doi.org/10.29303/spektrum.v9i2.239.

[31] Sholikhan, M., Prasetyo, S. Y. J. and Hartomo, K. D., (2019). Pemanfaatan WebGIS untuk Pemetaan Wilayah Rawan Longsor Kabupaten Boyolali dengan Metode Skoring dan Pembobotan [The Use of WebGIS for Mapping Landslide-Prone Areas in Boyolali Regency Using a Scoring and Weighting Method]. *Jurnal Teknik Informatika dan Sistem Informasi,* Vol. 5(1); 131-143. https://doi.org/10.28932/jutisi.v5i1.1588.

[32] Basri, H., Sufardi, S., Thomin, H., Syakur, S., Azmeri, A. and Hasan, H., (2023). Assessment of Drought Indices and Water Availability Using Statistical Z-Score and Mock Model. *Iraqi Journal of Agricultural Sciences,* Vol. 54(2); 388–398. https://doi.org/10.36103/ijas.v54i2.1713.

[33] Soerya, S. F., Asdak, C., Kendarto, D. R., Yan T. and Riyadi, A., (2023). F.J Mock Method for Hydrological Moel in Water Reliability Study in Leuwi Padjadjaran II Reservoir. *Journal of Advanced Zoology,* Vol. 44(5); 884-893. https://doi.org/10.53555/jaz.v44i5.3292.

[34] Chandrasasi, D., Montarcih Limantara, L. and Wulan Juni, R., (2020). Analysis Using the F. J. Mock Method for Calculation ff Water Balance in the Upper Konto Sub-Watershed. *IOP Conference Series: Earth and Environmental Science,* Vol. 437(1). https://doi.org/10.1088/1755-1315/437/1/012019.

[35] Seeboonruang, U., Mandadi, R., Thammaboribal, P., Gonzales, A. L.; Bharadwaz, G., S., V., S., A., (2025). Estimation of Soil Erosion and Enhancing Sediment Retention in the Lam Phra Phloeng Watershed: Insights from RUSLE and InVEST Modelling. *Water*, Vol. 17. https://doi.org/10.3390/w17233339.

[36] Ekawati, N., Danoedoro, P., and Wibowo, S. (2026). Erosion Rate Estimates in Relation to Land-use Change: A Case Study in Samin Watershed, Central Java, Indonesia. *International Journal of Geoinformatics*, Vol. 22(2), 80–96. https://doi.org/10.52939/ijg.v22i2.4789.

[37] Thammaboribal, P., Triapthti, N., and Lipiloet, S. (2025). Using of Analytical Hierarchy Process (AHP) in Disaster Management: A Review of Flooding and Landslide Susceptibility Mapping. *International Journal of Geoinformatics*, Vol. 21(4), 177–196. https://doi.org/10.52939/ijg.v21i4.4091.

[38] Al-Ghobari, H., Dewidar, A. and Alataway, A., (2020). Estimation of Surface Water Runoff for a Semi-Arid Area Using RS and GIS-Based SCS-CN Method. *Water,* Vol. 12(7). https://doi/org/10.3390/w12071924.

[39] Aditya, M. F., (2025). Estimasi Curve Number Daerah Aliran Sungai Konaweha Menggunakan Citra Satelit Dan Data Tanah Global [Estimation of the Curve Number for the Konaweha River Basin Using Satellite Imagery and Global Soil Data]. *SINERGI : Jurnal Riset Ilmiah,* Vol. 2(8); 3966–3978. https://doi.org/10.62335/sinergi.v2i8.1748.

[40] Satam, A., Mohammad, E., Najm, A., Mushref, Z., and Khalaf, A. (2025). Integration of Remote Sensing, GIS, and SCS-CN Model for Runoff Volume Estimation in Al-Deir Valley Basin, Iraqi Jazira Desert. *International Journal of Geoinformatics*, Vol. 21(9), 58–68. https:// doi.org/10.52939/ijg.v21i9.4443.

[41] Azizah, C., Pawitan, H., Nuraida, N., Satriawan, H., Abbas, R., Robo, S. and Misnawati, M., (2021) . Karakteristik Hidrologi dan Dampaknya Terhadap Banjir Daerah Aliran Sungai Jambo Aye di Aceh Indonesia [Hydrological Characteristics And Its Impact On Flood Jambo Aye Basin In Aceh Indonesia]. *Jurnal Penelitian Pengelolaan Daerah Aliran Sungai,* Vol. 5(2); 171–184. https://doi.org/10.20886/jppdas.2021.5.2.171-184.

[42] Mohd Yassin N. A., Adnan N. A. and Md Sadek, E. S. S., (2023). Analysis of Flash Flood Potential Index (Ffpi) and Scenarios Assessment in Shah Alam Using GIS Approach. *Planning Malaysia,* Vol. 21(2); 1-12. https://doi.org/10.21837/pm.v21i26.1255.

[43] Kocsis, I., Bilașco, Ș., Irimuș, I., Dohotar, V., Rusu, R. and Roșca, S., (2022). Flash Flood Vulnerability Mapping Based on FFPI Using GIS Spatial Analysis Case Study: Valea Rea Catchment Area, Romania. *Sensors (Basel, Switzerland),* Vol.22(9). https://doi.org/10.3390/s22093573.

[44] Chen, Z., Liu, X., Lu, Z. and Li, Y., (2021). The Expansion Mechanism of Rural Residential Land and Implications for Sustainable Regional Development: Evidence from the Baota District in China's Loess Plateau. *Land,* Vol. 10(2). https://doi.org/10.3390/land10020172.

[45] Nugroho, H. Y. S. H., Basuki, T. M., Pramono, I. B., Savitri, E., Purwanto, Indrawati, D. R., Wahyuningrum, N., Adi, R. N., Indrajaya, Y., Supangat, A. B. and Putra, P. B., (2022). Forty Years of Soil and Water Conservation Policy, Implementation, Research and Development in Indonesia: A Review. Sustainability, Vol. 14(5). https://doi.org/10.3390/su14052972.

[46] Shawaqfah, M., (2020). Mapping Flash Flood Potential and Risk Level Using GIS Techniques and the Flash Flood Potential Index (FFPI) in Amman Zarqa Basin of Jordan. *Jordanian Journal of Engineering and Chemical Industries,* Vol. 3(3); 81–90. https://doi.org/10.48103/jjeci3102020.

[47] Kulsoontornrat, J., and Puangkaew, N. (2025). Assessing the Impacts of Land Use and Land Cover Changes on Sediment Yield Using the SWAT Model: A Case Study in the Khlong Bang Yai Watershed, Phuket Island, Thailand. *International Journal of Geoinformatics*, Vol. 21(5), 62–79. https://doi.org/10.52939/ijg.v21i5.4161.

[48] Shi, Q., Wang, Q., Guo, W., Chen, Z., Feng, L. and Zhao, M., (2020). Response of the Headcut Erosion Process to Flow Energy Variation in the Loess Gully Region of China. *Water,* Vol. 14(9). https://doi.org/10.22541/au.159294164.40089465.

[49] Mardiansyah, W., Setiabudidaya, D., Khakim, M. Y. N., Yustian, I., Dahlan, Z. and Iskandar, I., (2018). On the Influence of Enso and IOD on Rainfall Variability Over the Musi Basin, South Sumatra. *Science and Technology Indonesia,* Vol. 3(4). https://doi.org/0.26554/sti.2018.3.4.157-163.

[50] Diop, M., Chirinda, N., Beniaich, A., El Gharous, M. and El Mejahed, K., (2022). Soil and Water Conservation in Africa: State of Play and Potential Role in Tackling Soil Degradation and Building Soil Health in Agricultural Lands. *Sustainability,* Vol. 14(20). https://doi.org/10.3390/su142013425.

[51] Silalahi, F. E. S., Arifianti, Y. and Hidayat, F., (2019). Landslide Susceptibility Assessment Using Frequency Ratio Model in Bogor, West Java, Indonesia. *Geoscience Letter,* Vol. 6(1). https://doi.org/10.1186/s40562-019-0140-4.

[52] Ely, S. S., Haumahu, J. P. and Ufie, C., (2023). Studi Perkembangan Tanah Pada Suatu Toposekuen di Negeri Assilulu Kecamatan Leihitu Kabupaten Maluku Tengah [A Study of Soil Development in a Toposequence in the Village of Assilulu, Leihitu Sub-district, Central Maluku Regency]. *Jurnal Agrosilvopasture-Technology,* Vol. 2(2); 524–530. https://doi.org/10.30598/j.agrosilvopasture-tech.2023.2.2.524.

[53] Carollo, F. G., Di Stefano, C., Nicosia, A., Palmeri, V., Pampalone, V. and Ferro, V., (2023) . New Strategy to Assure Compliance with Soil Loss Tolerance at a Regional Scale. *Catena,* Vol. 223. https://doi.org/10.1016/j.catena.2023.106945.

[54] Wijaksana, F. Kerugian akibat Banjir Bandang Garut Mencapai Rp 288,5 Miliar [Losses Caused By The Flash Floods in Garut Amount to Rp 288.5 billion]. Tribun News. [Online]. Available: https://jabar.tribunnews.com/2016/10/26/Kerugian-Akibat-Banjir-Bandang-Garut-Mencapai-Rp-2885-Miliar#:~:Text=Kisaran%20angkanya%20di%20Rp%20288%20miliar%2C%22%20ujar,Rp%2064%2C7%20miliar%20atau%2022%2C45%20persen%2C%20sektor. [Accessed: Nov. 28, 2025].